

Strength Degradation in Lead-Rubber Bearings during a Long-duration Earthquake

Tomotaka Wake

OILES Corporation, Ashikaga, Japan.

Masaru Kikuchi & Ken Ishii

Hokkaido University, Sapporo, Japan.



2017 NZSEE
Conference

ABSTRACT: A lead-rubber bearing (LRB) is one of the most common types of seismic isolation system. The strength of LRBs is reduced by “lead core heating” caused by their absorption of seismic energy. The purpose of this study is to resolve this issue of strength degradation afflicting the lead core in LRBs in the event of a long-duration earthquake. Accordingly, LRBs with two new types of structures are proposed. These newly improved LRBs were evaluated with dynamic-loading tests. The test program used subjected the LRB specimens to a deformation regime that can be expected in a long-duration earthquake. The test results show that the structurally improved LRBs out-perform regular LRBs. A new analysis method to predict the mechanical behaviour of the LRBs was also developed. A unique feature of the proposed method, which is coded in OpenSees, is its combination of seismic response analysis with heat-conductivity analysis. In particular, it interactively updates its parameters according to the temperature of the lead core (obtained from heat-conductivity analysis). The proposed analysis method was able to successfully predict the mechanical behaviour and temperature change for both types of LRBs observed in the loading tests. In other words, it can predict the mechanical behaviour of LRBs during a long-duration earthquake.

1 INTRODUCTION

The probability of very large subduction earthquakes in the Nankai and Tokai regions of Japan is of major concern in the Japanese earthquake-engineering community. Previous research has predicted that these events will produce long-duration, strong ground shaking with long-period characteristics. The energy absorption performance of LRBs is degraded by the temperature rise of the lead core caused by hysteretic energy absorption in the event of a long-duration earthquake, or in the cyclic loading test (Takenaka et al. 2009). Much experimental research has been performed to create a method of predicting the energy absorption degradation of LRBs, as this is detrimental to the safety of isolation structures (Kondo et al. 2008; Kalpakidis and Constantinou 2009). The purpose of this study is to develop a highly durable LRB by improving their energy absorption performance under cyclic loadings. As one approach, we propose two types of high heat capacity LRBs in this paper. Cyclic loading tests and heat-mechanics interaction analyses are conducted in order to show the improved performance of the proposed LRBs.

2 TEST SPECIMENS

The proposed lead-rubber bearings are shown in Figure 1. Type 1 is a regular type of LRB. Types 2 and 3 are high heat capacity LRBs with a different inner structure from Type 1, as shown in Table 1, so as

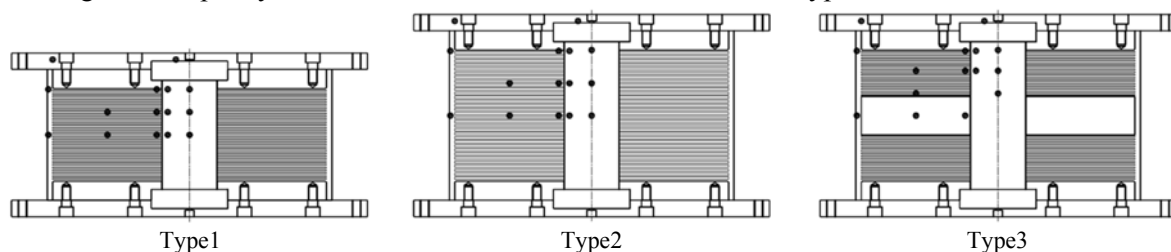


Figure 1. Cross sections of lead-rubber bearings (Type 1, Type 2, Type 3 from left)
Black markers on the cross sections indicate the positions of thermocouple sensors

to increase the heat capacity of the LRB. The inner thin plates of Type 2 have twice the thickness of the Type 1's inner plates. Types 1 and 3 have inner thin plates of the same thickness, but Type 3 has a thick inner plate to adjust the heat capacity to match that of Type 2. As a result of these changes, Types 2 and 3 have a heat capacity about 1.3 times that of Type 1. Many thermocouple sensors are installed in the LRBs for detailed assessment of the change in temperature of the LRBs.

3 EXPERIMENTAL CONDITIONS AND RESULTS

LRBs have been tested as per the conditions shown in Table 2 using 0.5-MN tri-axial testing apparatus. Assuming that each LRB is attached to a concrete structure, 12.7-mm thick heat insulators are installed on the outer ends of the flange plates. Because of the testing apparatus conditions, 2.5-MPa vertical loads were used in the tests, which were less than the design load of 15 MPa.

Table 1. Basic geometric parameters of lead-rubber bearings

| Parameters | Unit | Type 1 | Type 2 | Type 3 |
|------------------------|-------------------|-------------------------|-------------------------|--|
| Rubber hardness grade | N/mm ² | G0.4 | G0.4 | G0.4 |
| Rubber diameter | mm | φ500 | φ500 | φ500 |
| Lead core diameter | mm | φ100 | φ100 | φ100 |
| Rubber thickness | mm | 33 layers @ 3.0 = 99 | 33 layers @ 3.0 = 99 | 32 layers @ 3.0 + 2 layers @ 1.5 = 99 |
| Thin plate thickness | mm | 32 plates @ 2.2 | 32 plates @ 4.4 | 32 plates @ 2.2 |
| Thick plate thickness | mm | - | - | 1 plate @ 70.4 |
| End plate thickness | mm | 2 plates @ 35 | 2 plates @ 35 | 2 plates @ 35 |
| Flange plate thickness | mm | 2 plates @ 30 | 2 plates @ 30 | 2 plates @ 30 |

Table 2. Test conditions

| Experimental case | Vertical pressure | Amplitude of motion | Period of motion | Test cycles | Travel Distance |
|-------------------------|-------------------|---------------------|-------------------|-------------|-----------------|
| 1. Basic characteristic | 2.5 MPa | ±99 mm (±γ100%) | Sine wave 80 s | 4 | 1.6 m |
| 2. Cyclic loading | 2.5 MPa | ±198 mm (±γ200%) | Sine wave 4 s | 35 | 27.7 m |

3.1 Basic characteristic experiment

Recorded force-displacement hysteresis loops of basic characteristic tests (Case 1), and the rate of difference from the design value in terms of post-yield stiffness (Kd) and yield load (Qd), are presented in Figure 2. Although the yield load for Type 3 is a little larger than the others, each type of LRB demonstrated a steady bilinear hysteresis loop. In the basic characteristic experiments, we confirmed that the design currently used for regular LRBs can be applied to high heat capacity LRBs (Types 2 and 3) with revised inner structures.

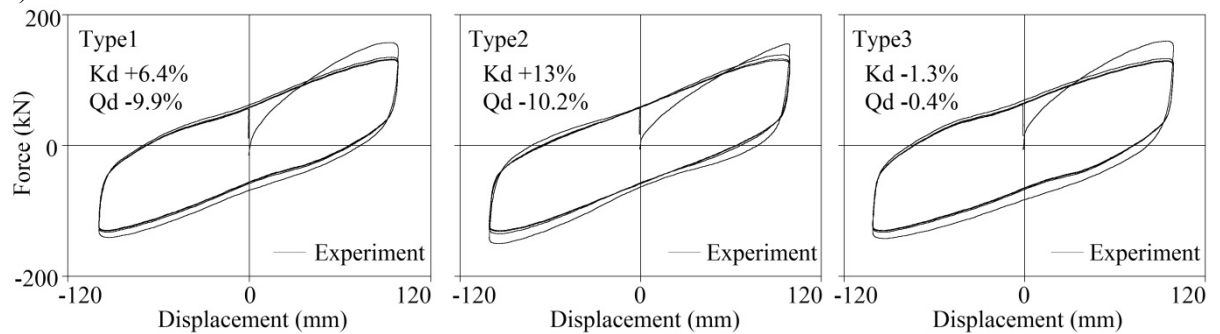


Figure 2. Force-displacement hysteresis loops obtained during basic characteristic tests

3.2 Cyclic loading experiment

The recorded force-displacement hysteresis loops of cyclic loading tests (Case 2) are presented in Figure 3. The characteristic strength and energy dissipated per cycle (EDC) for each type of LRB reduces as the cycles increase. The temperature histories for the centre of the lead core and rubber near the lead core, and the position of the sensors, are shown in Figures 4 and 5. The temperatures of the lead cores rose to 223°C in the case of Type 1, to 200°C for Type 2, and to 217°C for Type 3, respectively. The temperature of the rubber near the lead core rose to 81°C in the case of Type 1, to 51°C for Type 2, and to 47°C for Type 3, respectively. It took 12 minutes for the temperature of the test specimen to drop to 30°C in the case of Type 1, and 7 minutes for both Types 2 and 3. In the case of the high heat capacity LRBs, the temperature rise of both the lead core and rubber are reduced, and the temperature drop is faster than with regular LRBs.

Figure 6 presents the energy dissipated per cycle (EDC), and Figure 7 presents the cumulative energy dissipation histories for each type of LRB. The EDC for Type 2 and 3 represent the same value at the

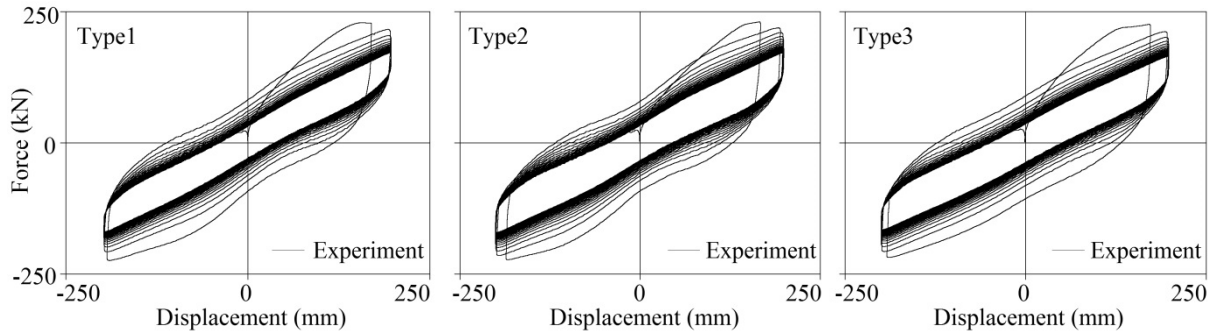


Figure 3. Force-displacement hysteresis loops during cyclic loading tests

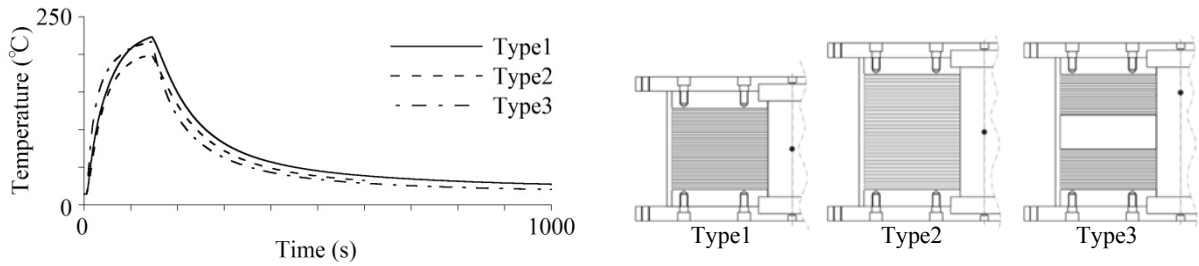


Figure 4. Lead core temperature histories obtained experimentally and positions of thermocouple sensors

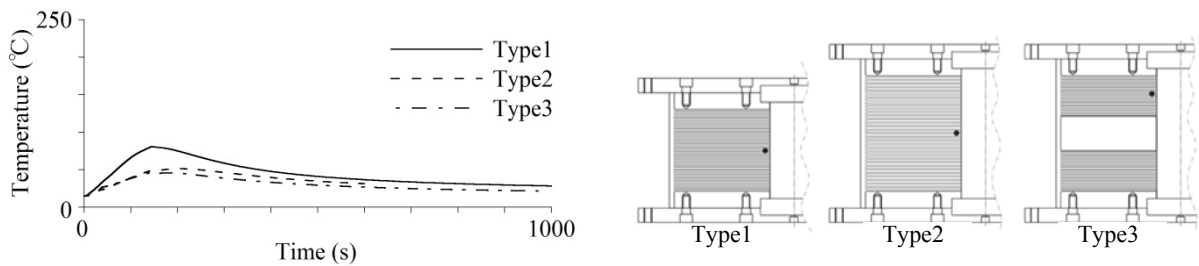


Figure 5. Rubber temperature histories obtained experimentally and positions of thermocouple sensors

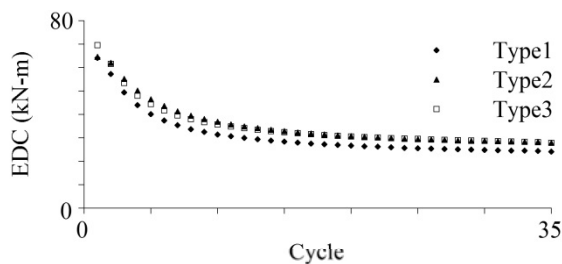


Figure 6. Energy dissipation per cycle

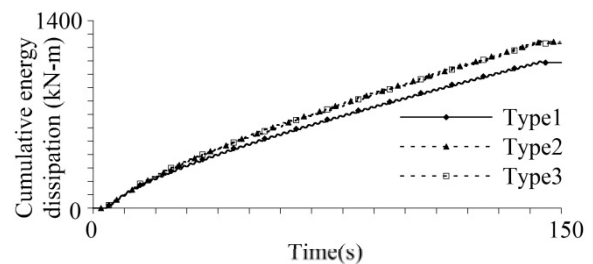


Figure 7. Cumulative energy dissipation

second cycle, while the EDC for Type 1 is lower than the others. Although the EDC for each type of LRB decreases gradually as the temperature of the lead core increases, the decrease in the EDC of Types 2 and 3 are lower than for Type 1. Cumulative energy dissipation for Types 2 and 3 was 13.9% and 12.7% improved, respectively, over Type 1. From the above, we confirmed experimentally that LRBs with improved heat capacity and heat dissipation characteristics were more effective in terms of reducing the rise in temperature of the lead core and increasing the cumulative energy dissipation.

4 METHOD OF HEAT-MECHANICS INTERACTION ANALYSIS

In order to express the heat-generating phenomenon of the lead core and the energy dissipation-reducing phenomenon of LRBs, the Kikuchi-Aiken model is introduced to finite volume method (FVM) non-stationary heat conduction analysis (Kikuchi and Aiken. 1997). This model can accurately predict the mechanical properties of LRB under a shear strain of up to 400%. The analysis model is implemented in the software program OpenSees.

The model for heat conduction analysis on Type 1 is shown in Figure 8. In order to model various inner structures, the thin plates and rubber layers are modelled separately. Table 3 presents the material properties used for the lead core, steel plates, rubber layers, and heat insulators.

The relationship between yield stress τ and lead core temperature T is used in Equation 1 below as shown in Figure 9 as obtained from previous experimental studies of LRBs (Kondo et al. 2009).

Figure 10 presents a flowchart of the heat-mechanics interaction analysis. FVM non-stationary heat conduction analysis updates interactively the temperature of lead core.

$$\tau = \tau_0 \left\{ 1 - \left(\frac{T}{T_L} \right)^{\alpha_T} \right\}, \quad \alpha_T = 0.4 + 0.25 \cdot \left(\frac{T}{T_L} \right) \quad (1)$$

$$\tau_0 = 15(\text{N/mm}^2), \quad T_L = 327.5 (\text{°C})$$

where τ_0 = yield stress of lead core at 0°C; T_L = melting point of lead.

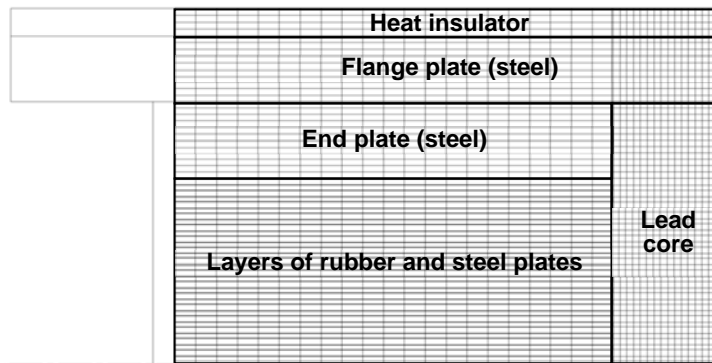


Figure 8. Axisymmetric finite-volume model for heat conduction analysis (Type 1)

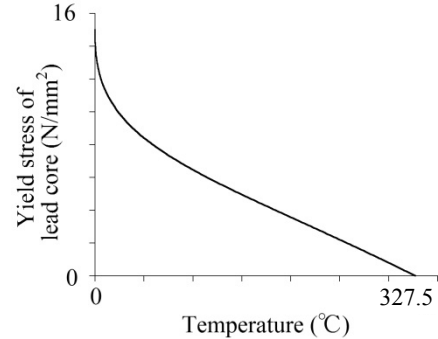


Figure 9. Relationship between yield stress and temperature of lead core

Table 3. Material parameters used in heat conduction finite-volume analysis

| Parameters | unit | Lead core | Steel plates | Rubber layers | Heat insulator |
|---------------|-------------------|-----------|--------------|---------------|----------------|
| Conductivity | W/(m-K) | 35.2 | 59 | 0.13 | 0.274 |
| Density | kg/m ³ | 11,330 | 7,860 | 1,040 | 2,050 |
| Specific heat | J/(kg-K) | 130 | 473 | 1900 | 931 |

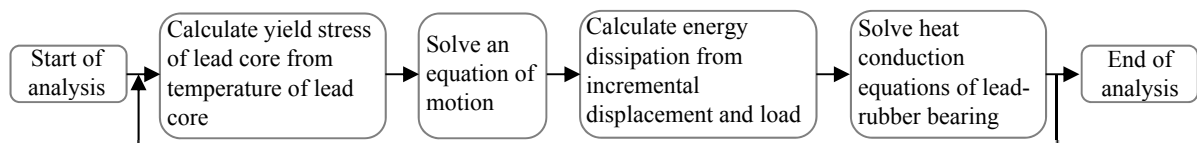


Figure 10. Flowchart of heat-mechanics interaction analysis

5 COMPARISON OF ANALYTICAL AND EXPERIMENTAL RESULTS

Figure 11 presents the recorded force-displacement hysteresis loops together with loops obtained by the heat-mechanics interaction analysis. Comparing the two results, the analytical model is capable of accurately predicting the degradation in energy absorption performance of the LRBs.

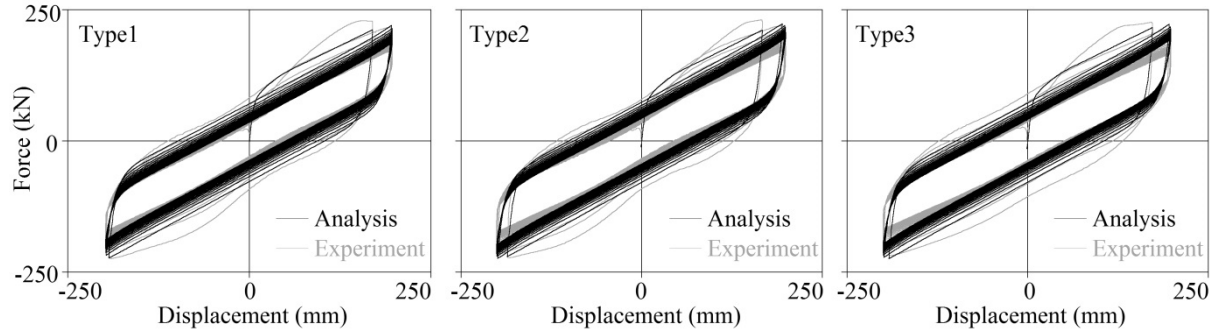


Figure 11. Comparison of analytically and experimentally obtained force-displacement hysteresis loops (Case 2)

The recorded and analysed temperature histories for Type 1 and the position of sensors are shown in Figure 12. Although two thermocouples (g and n) were destroyed by shear deformation, the temperature histories at many positions throughout the LRBs were obtained. Comparing the results, good agreement was obtained between the analytical and experimental results in almost all positions, not only for peak values, but also for the temperature increase process during loading and temperature decrease after loading. The recorded and analysed temperature histories and positions of the sensors for Types 2 and 3 are shown in Figures 13 and 14 respectively. The temperature of the rubber near the lead core obtained by analysis is larger than the experiment. Because the positions were at points where the temperature

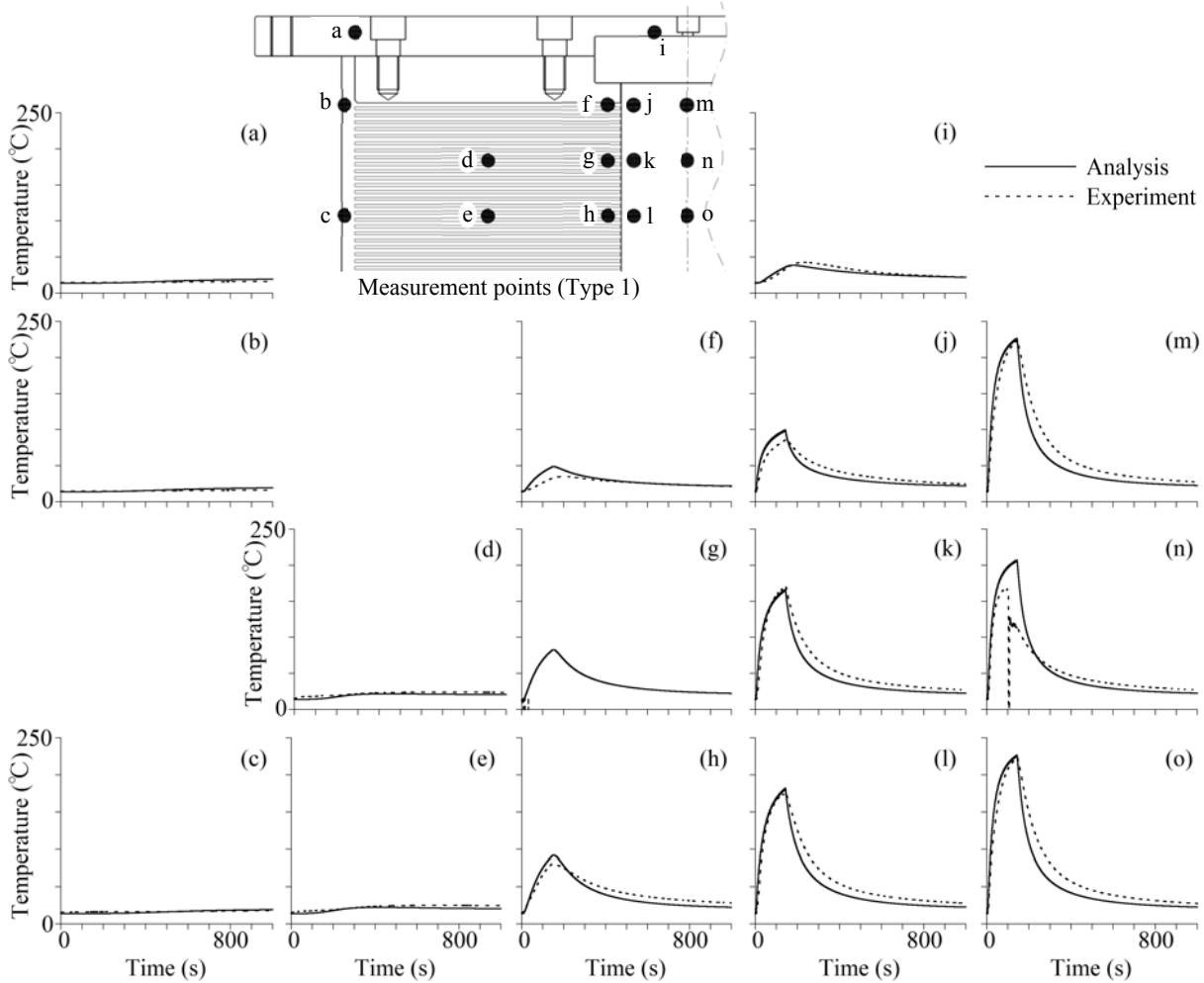


Figure 12. Comparison of analytically and experimentally obtained temperatures (Type 1, Case 2)

initially rose suddenly then tapered off, a slight shift in the position of the sensor can make a large difference in the results. Comparing the results, in the case of the LRBs with revised inner structures, good agreement was also obtained between the analytical and experimental results in the same manner as Type 1.

Figure 15 presents the EDC and Figure 16 presents the cumulative energy dissipation histories obtained experimentally together with those obtained from the heat-mechanics interaction analysis. The heat-mechanics interaction analysis can accurately express the degradation in the energy absorption performance of LRB.

Under analysis, the increase in cumulative energy dissipation for Types 2 and 3 over Type 1 was 15.6% and 9.3%, respectively. These results show good agreement with the experimental results, which were 13.9% and 12.7%, respectively.

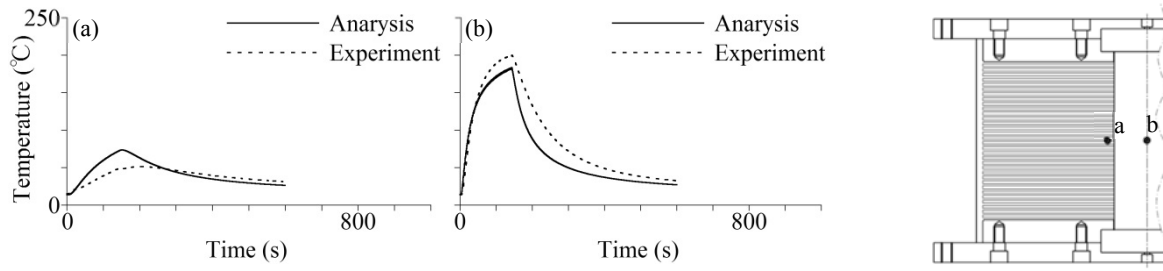


Figure 13. Comparison of analytically and experimentally obtained temperature histories and explanatory diagram of the measurement points (Type 2, Case 2)

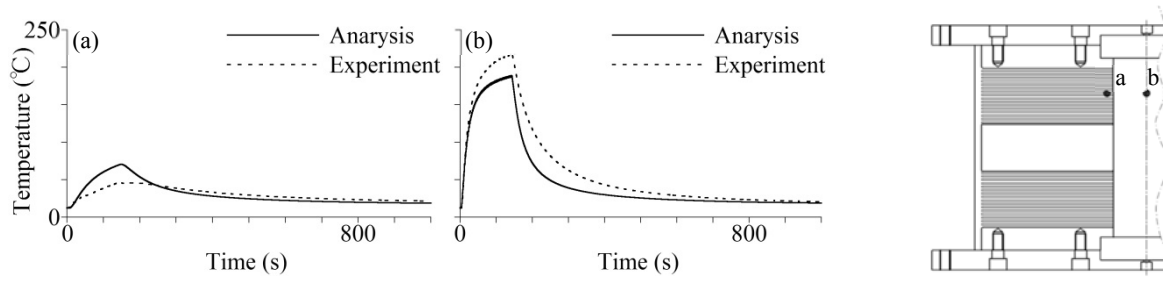


Figure 14. Comparison of analytically and experimentally obtained temperature histories and explanatory diagram of the measurement points (Type 3, Case 2)

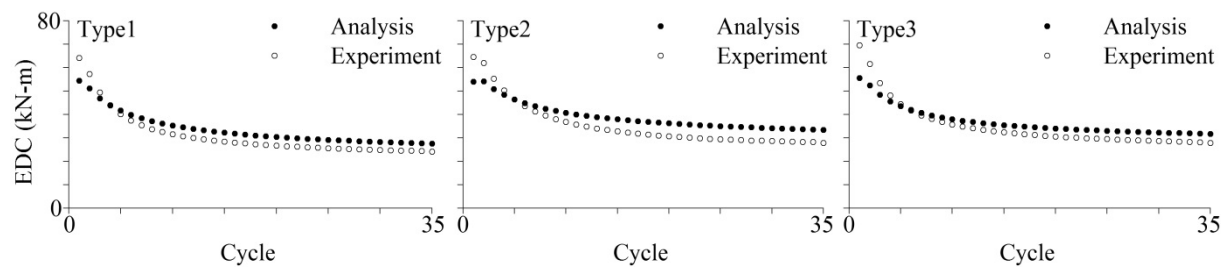


Figure 15. Comparison of analytically and experimentally obtained energy dissipation per cycle (Case 2)

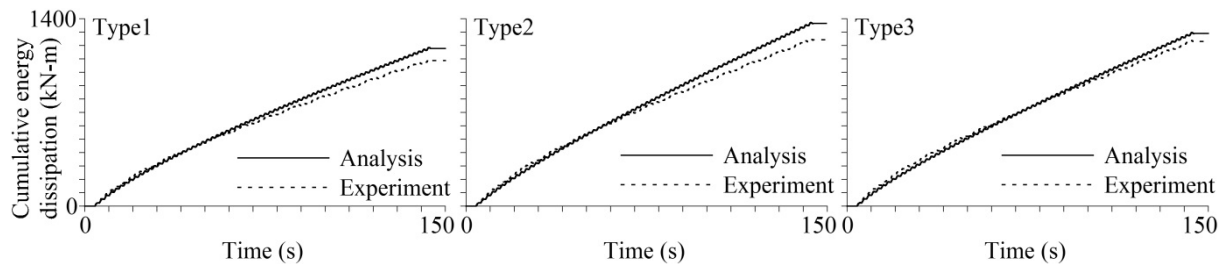


Figure 16. Comparison of analytically and experimentally obtained cumulative energy dissipation (Case 2)

Temperature distributions of LRBs obtained by analysis and experiment at the end of loading are presented in Figures 17 and 18. In vertical distribution, the temperature at the centre of the lateral deformation layers indicates the largest increase, and in horizontal distribution, the temperature is

decreased to the outer side in a radial direction. In horizontal distribution, a sudden drop in temperature at the outer peripheral surface of the lead core is indicated, and the temperature of the rubber near the lead core is reduced to almost half the temperature at the centre of the lead core. These results show good agreement with the experimental results.

From the above, we confirmed that the heat-mechanics interaction analysis is able to accurately express the effect of high heat capacity LRBs with improved heat capacity and heat dissipation characteristics, in terms of reducing the rise in temperature of the lead core and increased cumulative energy.

Figure 17. Vertical temperature distribution at the centre of lead-rubber bearings at the end of loading (Case 2)

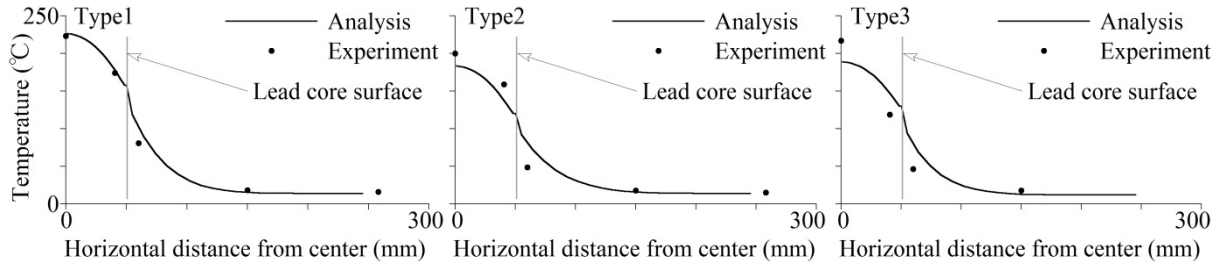
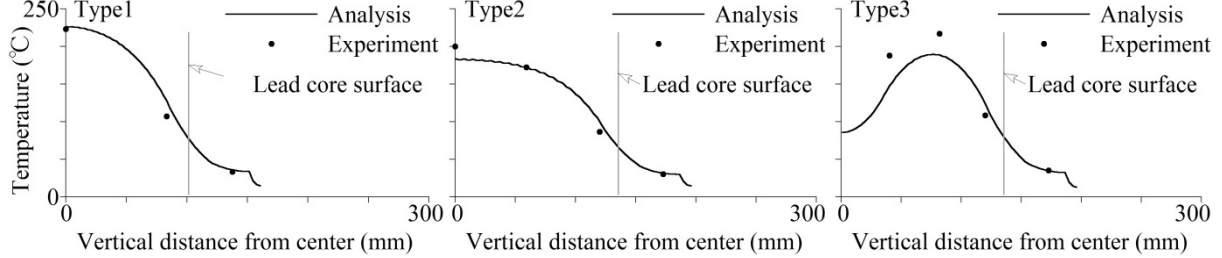


Figure 18. Horizontal temperature distribution at the centre of the stack of lateral deformation layers (Case 2)

6 SEISMIC RESPONSE ANALYSIS OF ISOLATED STRUCTURE

The validity of the heat-mechanics interaction analysis is confirmed from the above. We applied the analysis to a model of an isolated building installed with full-scale LRBs. The building is modelled as a 15-storey mass system structure with 16 LRBs installed with a diameter of 1,000 mm, which are double

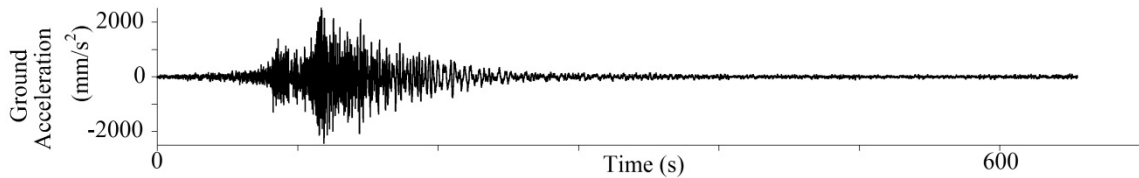


Figure 19. Time history of input ground motions

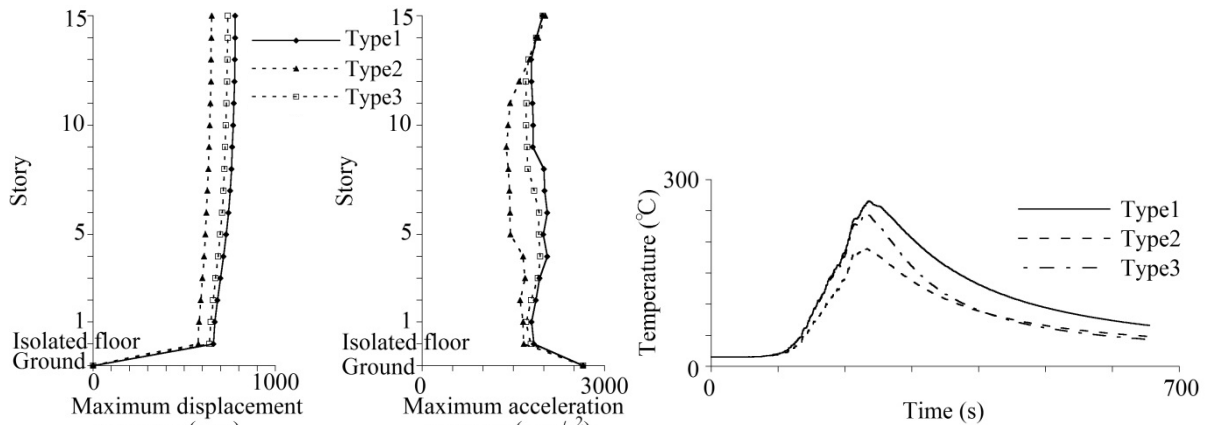


Figure 20. Distributions of peak response values

Figure 21. Time history of temperature at the centre of lead core

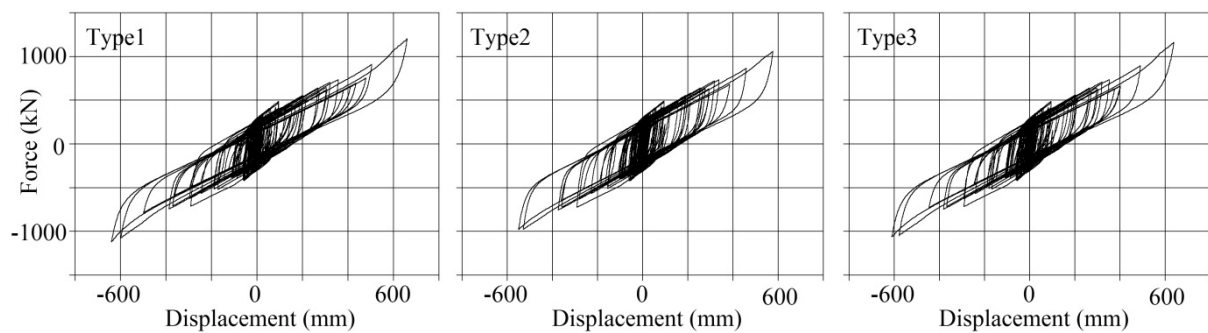


Figure 22. Force-displacement hysteresis loops

the size of the LRB shown in Figure 1. The ground motion used for analysis assumes a long-duration earthquake as shown in Figure 19.

The distribution of maximum response acceleration and displacement is presented in Figure 20. The high heat capacity LRBs, especially Type 2, effectively reduce both the acceleration response and displacement response in comparison with Type 1. The maximum temperature of Type 2 was 76°C less than Type 1, as shown in Figure 21. Figure 22 presents the force-displacement hysteresis loops. The maximum response displacement for Type 2 was 82.5 mm less than Type 1 (i.e. about 42% in shear strain). The difference in response between Type 2 and Type 3 reflects the arrangement of high capacity inner plates. The positions of the high capacity inner plates in Type 2 are closer to the high temperature part of the lead core than the position used in Type 3. This arrangement is effective for reducing the temperature of the lead core and the degradation in energy absorption performance.

7 CONCLUSION

We experimented on high heat capacity LRBs with improved heat capacity and heat dissipation characteristics designed to handle a long-duration earthquake. In order to grasp the effectiveness of high heat capacity LRBs, we developed a heat-mechanics interaction analysis and compared them with the experimental results, and analysed an isolated structure with full-scale LRBs installed in the event of a long-duration earthquake. The basic characteristics of high heat capacity LRBs are the same as regular LRBs, so the design of the regular LRB can be applied to high heat capacity LRBs. The heat-mechanics interaction analysis that we developed can accurately express the effect of high heat capacity LRBs in terms of the reduction in the rise in temperature of the lead core and increased cumulative energy. From the analytical response simulation, the high heat capacity LRB effectively reduces both the response acceleration and response displacement.

ACKNOWLEDGEMENTS

This research was partially supported by the Japan Society for the Promotion of Science, Grant-in-Aid for Scientific Research (A), 15H02274, 2016. Dr. Frank McKenna of the University of California, Berkeley, U.S.A., assisted in the implementation of the analytical models in the OpenSees program. The authors would like to express their thanks for all support and contributions.

References

- Takenaka et.al, Experimental study on heat-mechanics interaction behaviour of laminated rubber bearings: J. Struct. Constr. Eng., AIJ, Vol. 74 No. 646, 2245-2253, Dec., 2009 (in Japanese)
- Kondo et.al, Heat-Mechanics Interaction Behaviour of Laminated Rubber Bearings under Large and Cyclic Lateral Deformation (Part 10: Proposal of Relationship between Temperature and Shear Stress of Lead core), Summaries of Technical Papers of Annual Meeting of AIJ, Structure II, pp. 399-400, 2008.9 (in Japanese)
- Kalpakidis IV, Constantinou MC (2009) Effects of heating on the behavior of lead-rubber bearings, I: theory. ASCE. J Struct Eng 135(12): 1440-1449
- Masaru Kikuchi, Ian Aiken, 'An Analytical Hysteresis Model for Elastomeric Seismic Isolation Bearings', EESD, Vol. 26, 215-231, 1997